RESEARCH ARTICLE

Macromolecular Bioscience
www.mbs-journal.de

Application of Temporary, Cell-Containing Alginate Microcarriers to Facilitate the Fabrication of Spatially Defined Cell Pockets in 3D Collagen Hydrogels

Sarah Lehnert and Pawel Sikorski*

Mimicking the complexity of natural tissue is a major challenge in the field of tissue engineering. Here, a facile 2-step fabrication method to prepare 3D constructs with distinct regions of high cell concentrations and without the need for elaborate equipment is proposed. The initial incorporation of cells in a sacrificial alginate matrix allows the addition of other, cell relevant biopolymers, such as, collagen to form a spatially confined, interpenetrating network at the microscale. A layered structure at the macroscale can be achieved by incorporating these cell-containing microspheres in thin collagen layers. Cells are locally released by de-gelling the alginate matrix and their attachment to the collagen hydrogel layers has been studied. The use of the murine pre-osteoblast cell line MC3T3-E1 as an example cell line shows that the cells behave differently in their cell migration pattern based on the initial composition of the alginate microspheres.

1. Introduction

Biological tissues such as bone are heterogeneous and complex across length scales ranging from nanometer to millimeter.[1–3] The extracellular matrix (ECM) that surrounds the tissue-specific cells varies in its biochemical composition and physical characteristics such as stiffness and elasticity and plays an active role in guiding, restraining, and anchoring cells.[4–6] The ECM is a constantly changing, hierarchically organized network consisting of growth factors,[7] soluble and insoluble proteins,[8,9] and biopolymers which form the mechanical framework. Even for one tissue, the ECM is heterogeneously constructed, providing chemical and physical cues for the incorporated cells.[10,11]

The aim of tissue engineering (TE) is the development of 3D tissue in vitro for the restoration and maintenance of functions for injured, damaged or diseased counterparts in vivo.[12] But also the application of such constructs as 3D model systems to study the progression of diseases or the impact of drugs in vitro is of great interest.[13,14] However, the complexity of tissue is difficult to mimic in vitro. In vivo, cues in the ECM regulate cellular processes such as migration, proliferation, and differentiation.[15–17] Being able to mimic these is a critical aspect needed for the successful development of large-scale 3D tissue constructs in vitro. Considering the complexity of biological tissue, it is necessary to develop artificial model systems that are more complex and can recapitulate the ECM better in all its diversity, this includes controlling local biochemical and mechanical cues, as well as, the cell type and the local cell density. The general approach in TE involves the use or development of a scaffold which exhibits certain mechanical, biochemical, or physical cues and the subsequent seeding and studying of cells.

The first steps of evaluating artificial, in vitro constructs are to look at the cell adhesion, their adaption to the environment and, consequently, their migration into the surrounding material. To study the cell migration in 3D in particular, several assays can be found in the literature. Both, the Boyden chamber[18,19] and gel invasion method,[20,21] are comprised of applying a cell suspension on top of the construct and consequently recording the migration of cells into the constructs due to chemotaxis or other fabricated gradients. Furthermore, the gel invasion method is not only used for soft, hydrogel-based, scaffolds but also often for rigid scaffolds prepared by freeze-drying[22] or cell-free 3D-printing.[23] In contrast to these two methods, facilitates the radial assay the dispersion of cells in a 3D hydrogel matrix. Here, cells are attached to the outer surface of microcarriers before being embedded in a hydrogel material and the radial progression of the cells into the surrounding material is captured. The use of disks[24,25] or spherical microcarriers have been reported.[26–28] The conducted studies with microcarriers differ in the initial materials of the microcarriers, the origin of the surrounding hydrogels as well as the choice of cells. However, they all have in common that the colonization of the microcarriers with cells took between 4 and 14 days and no active interference has been initiated to dissolve or remove the microcarrier substrates from the constructs once the cells started migrating.[27,28]

Hydrogels are a well-established class of materials that are used to mimic ECM in vitro.[29–32] They are 3D networks of

S. Lehnert, P. Sikorski
Department of Physics
Norwegian University of Science and Technology (NTNU)
Høgskoleringen 5, Trondheim 7034, Norway
E-mail: sarah.lehnert@ntnu.no

The ORCID identification number(s) for the author(s) of this article can be found under https://doi.org/10.1002/mabi.202100319

DOI: 10.1002/mabi.202100319

hydrophilic polymers that are cross-linked by chemical or physical means and that have a very high-water content. They can be made from both, synthetic and natural polymers.[33] Natural polymers commonly used for applications in tissue engineering are collagen, alginate, gelatin, hyaluronic acid, fibrin, as well as, a combination of polymers.[29,34–36] The specific choice of polymer system depends on the type of tissue that is in focus of the research and the associated physical and biochemical characteristics.

Alginate is an anionic polysaccharide at neutral pH which naturally occurs in brown seaweed. It is of particular interest for TE applications as it is biocompatible and non-toxic, enabling the encapsulation of cells.[37–39] Alginate consists of two block copolymers, (1,4)-linked β-mannuronate (M) and α-L-guluronate (G) residues. Especially the latter is responsible for the gentle gelation with multivalent cations such as calcium (Ca^{2+}) or barium (Ba^{2+}), following the so-called eggbox model and forming a crosslinked hydrogel.[40,41]

Collagens describe a group of triple helical proteins which have crucial roles in tissue assembly and tissue maintenance, including cell migration, tissue morphogenesis, and repair. In vivo, at least 28 different collagens exist and can be divided into fibril-forming collagens, such as collagen I and II (present in connective tissues) and network-forming collagens such as collagen IV (predominantly in basement membranes).[42–44] The in vivo synthesis and assembly of collagen is a complex process that results in tissues which vary in their mechanical characteristics. For instance; collagen type I represents roughly 90% of the organic mass of bone tissue which is among the stiffest natural tissues.[43,45] However, in vitro reconstituted collagen lacks the sufficient strength compared to native tissue. The self-assembly process depends on the pH, temperature and is also considered to be rather slow.[46–49]

The precise positioning of cells in a multi-layered, 3D hydrogel construct is mostly achieved by the use of 3D bioprinting.[50–52] The term describes an additive manufacturing technique with which the fabrication of highly complex architectures can be achieved. To date, three types of bioprinting are applied in the field of tissue engineering; droplet bioprinting,[53] laser bioprinting,[54] and the most commonly used extrusion bioprinting.[55] All three have in common that the cells are dispersed in so-called bioink. This material does not only incorporate and facilitate the distribution of cells in the construct, but it also serves as initial ECM for the cells. Hence, much consideration has been put in the choice and development of the specific bioinks.[56–58]

In this work, we present a 2-step method which allows the fabrication of 3D collagen constructs with distinct cell-containing pockets. Cells are immobilized in alginate microspheres which are consequently incorporated in a 3D collagen hydrogel. Upon gentle de-gelling of the alginate, the cells are released and start interacting with the surrounding collagen matrix, creating distinct cell pockets in the sample with a varying microstructure. Two types of microspheres as temporal cell microcarriers were used, pure alginate microspheres and alginate-collagen microspheres which resulted in distinctively, spatially different cell distributions and microenvironments. The use of alginate-collagen microspheres is hypothesized to retain the encapsulated cells after the dissolution of alginate and creating a collagen-based microenvironment. In contrast, pure alginate microspheres are expected to release the cells in the resulting void after dissolution.

For the proof-of-principle, the pre-osteoblastic murine cell line MC3T3-E1 (subclone 4) has been selected as model cell line. The fabricated constructs were characterized prior to alginate dissolution, during cell release, for ten days in culture and after the end of the culture period. We use second harmonic imaging microscopy (SHIM) to study structure development of collagen fibers in the constructs and confocal laser scanning microscopy (CLSM) to image the temporal distribution and migration of the cells. These cell–cell and cell–collagen matrix interactions were also investigated.

2. Results and Discussion

2.1. Construct Fabrication, Characterization of De-Gelling Mechanism and Cell Release

The aim of this study is to fabricate cell containing collagen hydrogels constructs with a locally enriched cell concentration. Employed fabrication process is illustrated schematically in **Figure 1**A. We investigate cells that are delivered in 0.6 wt% alginate (Alg) and in 0.6 wt% alginate-0.07 wt% collagen (AlgCol) microspheres and compare with constructs in which cells have been directly suspended in a collagen matrix. All constructs are prepared in molds (diameter: 8.5 mm) filled with collagen solution containing microspheres or suspended cells. In addition, a thin collagen layer is included at the bottom of the construct. It is used to hinder the contact between microspheres or cells and the bottom of the mold. In the presented cell delivery concept, alginate is used as a temporary cell carrier.

After the cell encapsulation step, microsphere size and number of cells per microsphere were measured (Figure 1B,C, respectively). Microsphere diameter ($\pm$ standard deviation (SD)) for Alg- and AlgCol microspheres were in the range of 650 ± 42 µm and 640 ± 40 µm, respectively, and each microsphere type contained 180 ± 35 and 188 ± 22 cells, respectively.

Ethylenediaminetetraacetic acid (EDTA) was used to de-gel alginate hydrogel and release encapsulated cells (**Figure 2**). EDTA is a chelating agent with a high affinity for calcium ions.[59,60] The cytotoxicity of EDTA depends on a multitude of factors such as, the cell type, EDTA concentration, and the incubation time. In general, the survival rate of cells decreases drastically for incubation periods longer than 20 min.[60–62] Following literature protocols, we have used 50 mM EDTA in pre-warmed phosphate buffered saline (PBS) and a treatment time below 10 min.[63–66] For both sample types, the de-gelling took ≈7 min. The progression of the de-gelling front can be followed by observing the decrease of opacity of the entrapped microspheres over time. Cells released from Alg-microspheres (Figure 2A) drifted toward the surrounding collagen hydrogel and on the periphery of the void created by dissolution of the alginate. This is further illustrated in Figure S1A, Supporting Information, which shows that cells accumulated at the interface to the surrounding collagen hydrogel (yellow arrows). In contrast, the cells that were encapsulated in AlgCol-microspheres are held in place by the collagen matrix in the alginate-collagen composite and do not drift when the alginate hydrogel is dissolved with EDTA (Figure 2B and Figure S1B, Supporting Information).

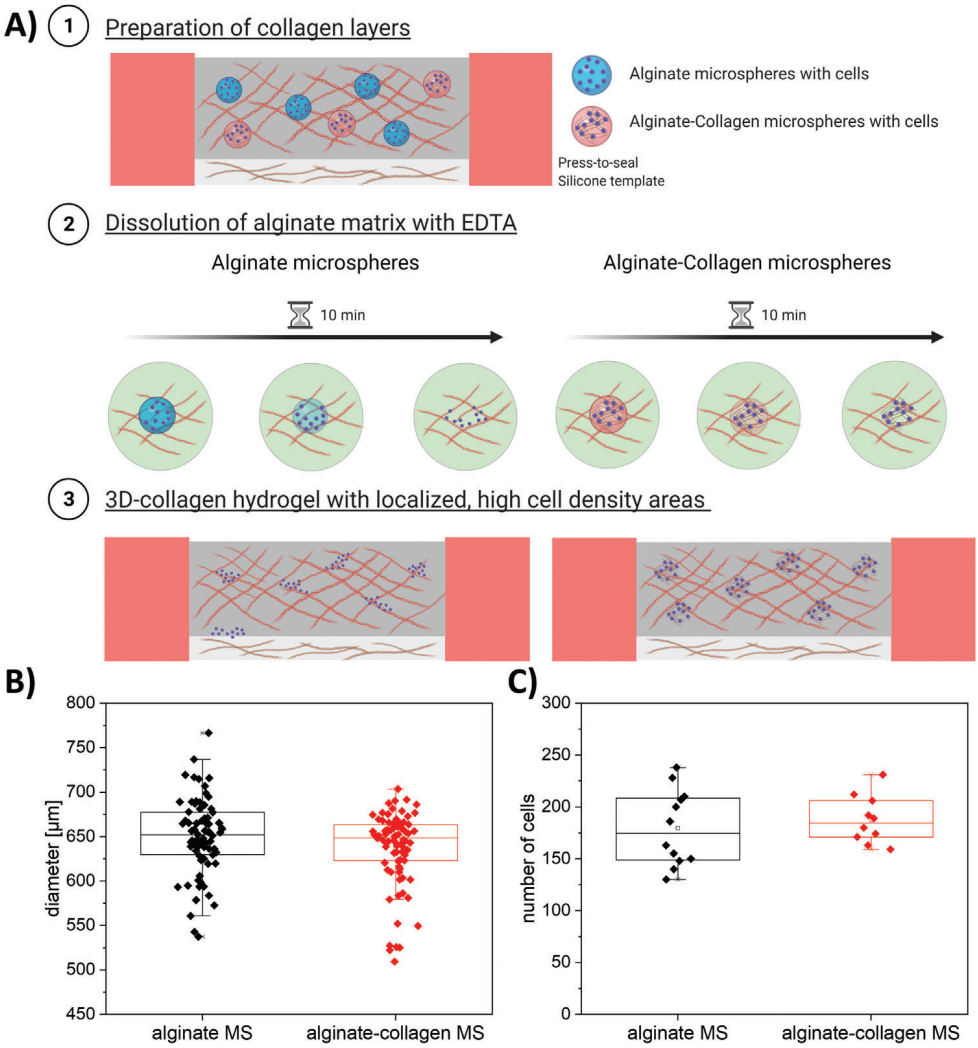

Figure 1. A) Schematic illustration of 3D construct fabrication process using cells encapsulated in alginate (Alg, blue) or alginate-collagen microspheres (AlgCol, red). Constructs are prepared within dents defined by press-to-seal silicon molds (dark red, diameter: 8.5 mm, depth 1.7 mm). The mold is first filled with collagen solution to form a thin collagen barrier that prevents the cells in the construct to contact the glass bottom of the wellplate. The mold is then filled by another collagen solution containing either alginate (Alg) or alginate-collagen (AlgCol) microspheres (see panel A.1). After 1 day, the alginate component is dissolved with EDTA (see panel A.2), allowing encapsulated cells to migrate into the 3D collagen hydrogel (panel A.3). B) Box plots of measured diameters of prepared microspheres prior to fabrication of the constructs. Median value is highlighted by horizontal line within each respective box and the whiskers indicate the smallest and the largest observed value. Values out of the range of the whiskers constitute calculated outliers. C) Box plots of cell-count per microsphere for Alg and AlgCol microspheres. Median value is highlighted by horizontal line within each respective box and the whiskers indicate the smallest and the largest observed value.

A follow-up characterization with two-photon microscopy is shown in **Figure 3**. After alginate dissolution, the samples were kept in cell media in the incubator for 20 min prior to imaging. Similarly, to the observation in Figures 2A and 3A confirms that initially released cells from alginate microspheres accumulated at the interface to the surrounding collagen hydrogel. The void that has been left by the dissolved alginate is clearly visible. In contrast, and in good agreement with the observations from Figure 2B, cells released from alginate-collagen microspheres are distributed uniformly throughout the former microsphere that, after de-gelling, is composed of collagen fibers previously assembled upon microsphere preparation. Although no clear void is detectable, the position of the microsphere can be detected by the difference in collagen fiber structure. SHIM relies on the intrinsic properties of assembled collagen fibers.[67] Assembled collagen type I fibers are made of ordered triple helix structure which fulfills the requirement of non-centrosymmetry.[68,69] SHIM showed that the collagen fibers assembled within the alginate-collagen microsphere had a morphology that was different from the surrounding collagen fibers (see Figure 3B). The assembly the collagen hydrogel used as a surrounding matrix for the microspheres, reflects an unhindered in vitro assembly of collagen fibrils.[70] Resulting collagen fibers show a fibrillar morphology with parallel fibers (see surrounding collagen hydrogel network in Figure 3A,B). The collagen fiber assembly within the microspheres was influenced by the alginate gelling process.[71] The collagen in the microspheres assembled into much shorter fiber bundles (Figure 3B, yellow arrows). According to Lutz et al.,

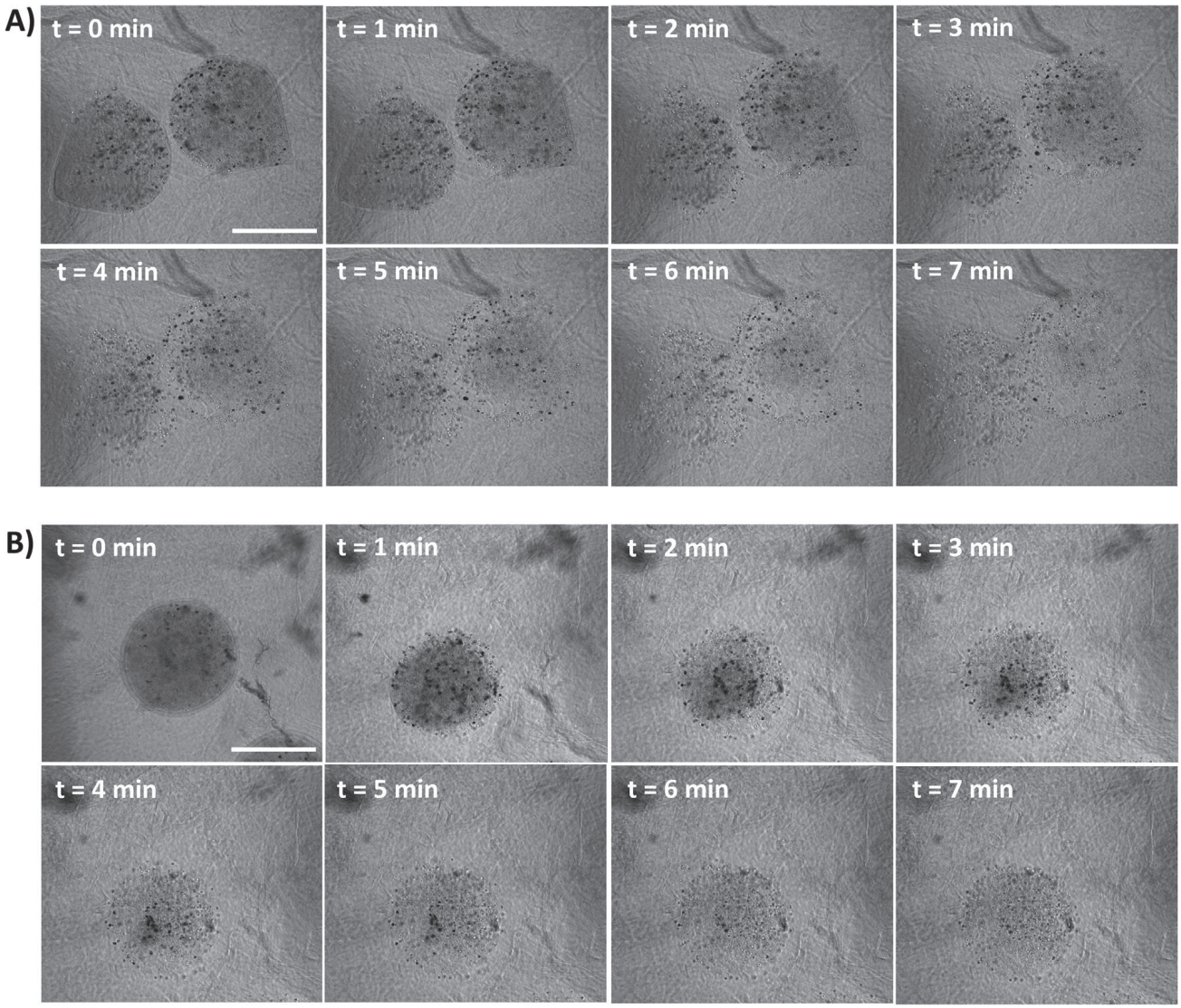

Figure 2. Time series of the alginate de-gelling process for cell-containing microspheres embedded in 3D collagen constructs. Data for A) Alg- and B) AlgColl- microspheres is presented. De-gelling is induced with EDTA that chelates the calcium ions which have crosslinked the alginate hydrogel upon microsphere preparation. Dissolution is visible by a change in microsphere opacity and is completed in about 7 min. Scale bar: 250 µm

a reduced collagen crosslinking results in collagen fibers with a curly morphology and with the fibers being less aligned to each other.[72] This description is in good agreement with our own observations, but the assembled collagen network is sufficiently stable to provide mechanical support for encapsulated cells.

2.2. Cell Migration in 3D Collagen Hydrogel Constructs

Alginate hydrogels are de-gelled with EDTA one day after preparation of collagen constructs. The de-gelling of the alginate matrix is marked as "Day 0" in the following section. The type of microsphere used for construct fabrication had a significant impact on observed cell migration, cell–cell interactions, and evolution of the construct morphology in culture. Cells released from alginate microspheres sedimented and settled at the bottom of the void within 2 days (**Figure 4**A, Figure S4, Supporting Information, (alginate MS)). At day 4, a significant number of cells migrated into the surrounding collagen hydrogel and started to interact with cells released from neighboring alginate microspheres (see Figure 4A). At day 8, the location of the void bottom is still visible by the presence of an increased cell concentration (Figure 4A) and there are distinct regions that facilitate cell–cell interactions for cells that were originally encapsulated in individual microspheres. In contrast, cells that have been encapsulated in alginate-collagen microspheres do not migrate as quickly into the surrounding collagen matrix (see Figure 4B, Figure S4, Supporting Information, (alginate-collagen MS)). On day 4, cell–cell interactions are observed for cells originating from the same microsphere (further highlighted in Figure S3, Supporting Information, orange arrows), and by day 8 these cells also started to migrate into the surrounding collagen matrix (see Figure 4B). Additional bright field images in Figure S3, Supporting Information, also imply the fundamental differences in the construct

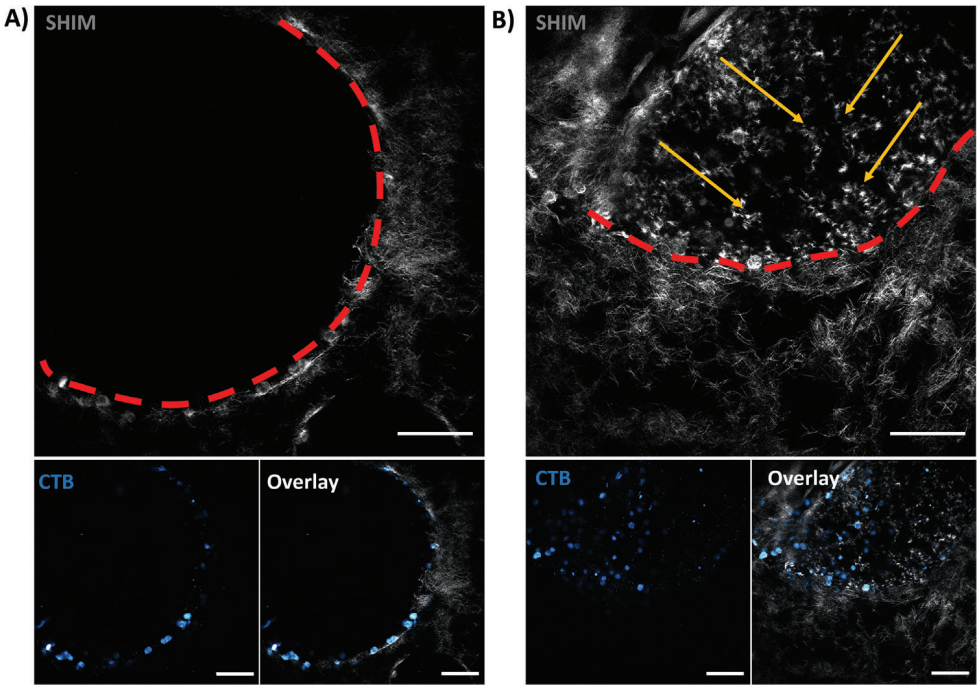

Figure 3. Visualization of collagen hydrogel constructs containing dissolved A) Alg and B) AlgCol microspheres right after dissolution. Collagen fibers have been imaged using SHIM (gray) and cells have been labeled using the Cell Tracker Blue (CTB, cyan). The edges of the microspheres that were present before de-gelling have been illustrated with a red dash line. The different structure of assembled collagen fibers in the microspheres is highlighted by the yellow arrows. Clear differences of the spatial distribution of cells between the two sample types can be observed. For Alg samples, cells drifted to the interface with the collagen hydrogel, and, for AlgCol microspheres, cells are kept in position by collagen hydrogel formed upon microsphere gelation process. Scale bar: 100 µm.

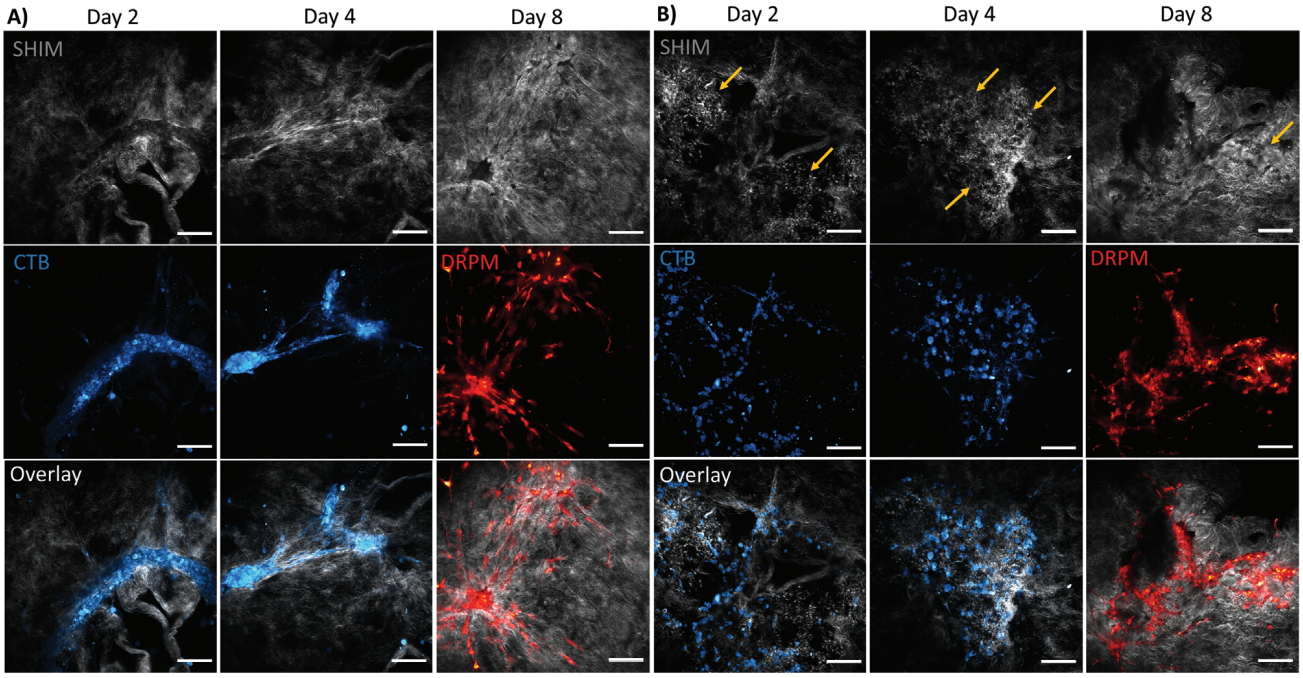

Figure 4. Visualization of MC3T3-E1 cells released from A) Alg and B) AlgCol microspheres. Surrounding collagen matrix consisted of 0.07 wt% collagen and all samples were immersed in regular cell media, without additional ascorbic acid or beta-glycerophosphate. Structural changes of the collagen network have been imaged using multiphoton microscopy (SHIM signal, gray). Arrows in section (B) highlight the apparent structural differences in the assembled collagen fibers in a microsphere setup. The ability of the cells to spread within the surrounding matrix has been imaged using two-photon fluorescence microscopy using Cell Tracker Blue (CTB, cyan) for the first four days of culture and using confocal laser scanning microscopy and Cell Mask Deep Red Plasma Membrane dye (DRPM, red) for the remaining days of the experiments. Scale bars: 100 µm.

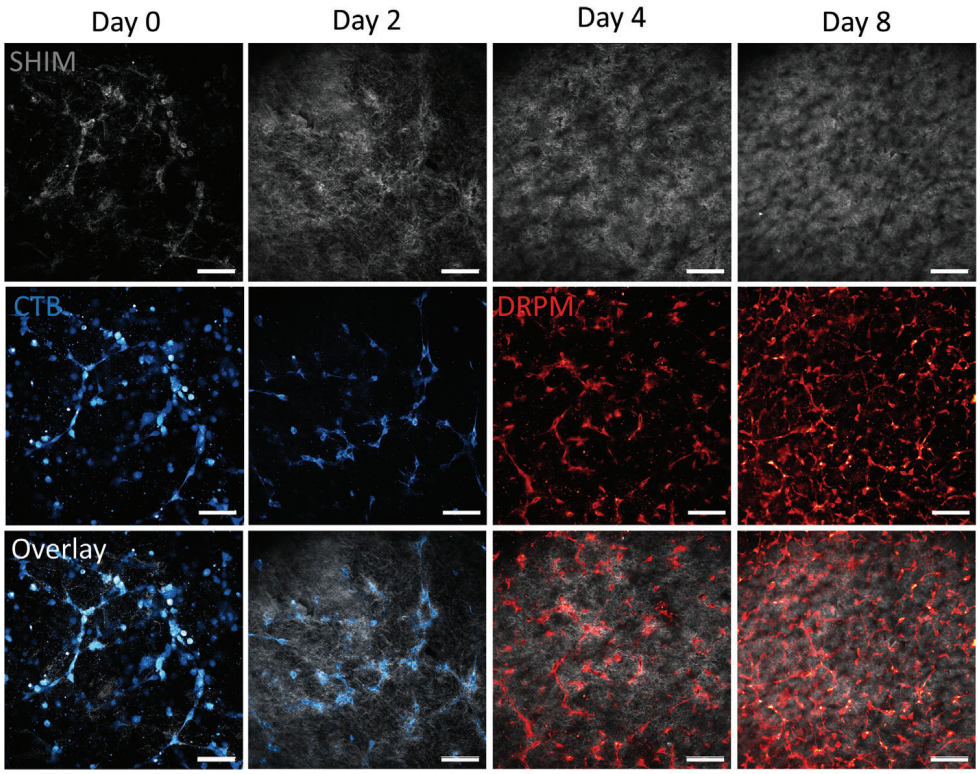

Figure 5. Structural changes of 0.07 wt% collagen hydrogel network containing evenly distributed MC3T3-E1 cells with a cell concentration of 50 000 cells mL^{-1} during eight days in culture. Collagen network has been imaged using SHIM (gray) and the cells contained the long-term cytosol Cell Tracker Blue (CTB, cyan) for the first 4 days of culture and using confocal laser scanning microscopy and Cell Mask Deep Red Plasma Membrane dye (DRPM, red) for the remaining days of the experiments as CTB faded over time. Scale bar: 100 µm.

geometries. The microsphere shape is well defined for the former alginate-collagen microspheres with the cells interacting within this region.

The increasing cell migration over time also had a direct impact on the organization of the surrounding collagen fiber matrix which was characterized SHIM microscopy. For the construct containing cells released from alginate microspheres, the origin of the voids made by the dissolved and collapsed alginate matrix remained detectable in the collagen network (Figure 4A, SHIM signal). The SHIM micrograph for the collagen network on day 8 shows that the collagen fibers in proximity of the cells appear brighter and more densely packed, suggesting that the cells locally contract their surrounding collagen matrix. In contrast, the collagen fibers from the alginate-collagen microspheres and the fibers assembled in the surrounding collagen hydrogel are clearly distinguishable throughout the culture period. Dissolution of the alginate or alginate-collagen microspheres had no significant effect on the overall structure of the constructs. Local voids created by alginate microspheres collapsed over time (Figures 3A and 4A), while the structure of the construct remained stable for the case of alginate-collagen microspheres (Figures 3B and 4B). In this case, the collagen component of the microspheres served as retaining scaffold for the encapsulated cells. In a control study in which the alginate in the microspheres were not dissolved, cells did not migrate into the surrounding collagen hydrogel in the course of the experiment (Figure S2, Supporting Information).

Next, the effect of locally released cells compared to uniformly distributed cells in collagen hydrogels has been investigated. Collagen hydrogels with a concentration of 0.07 wt% containing uniformly distributed MC3T3-E1 pre-osteoblastic cells were prepared. Cells were cultured in ascorbic acid-free cell media for eight days. **Figure 5** illustrates the SHIM signals for the assembled collagen fibers and the fluorescent cell stains for this timescale. Over time, the cells connect to each other, forming cell–cell-contacts and, by day 8, appear to start forming a network. After casting the cell–collagen solution into the mold, the collected SHIM signal shows that the collagen starts assembling close to and around the cells first (Figure 5, Day 0). The SHIM signals show that, after the initial assembly, there are small, visible pockets in the collagen hydrogel where the cells are located (Figure 5, Day 2). In the following 6 days, the collected SHIM signal shows that the collagen fiber network becomes more and more densely packed. The increased density of the collagen fibers is most likely due to the know effect of collagen hydrogel contraction. A characteristic process that has been previously reported for fibroblasts[73] and plays an important role in research focused on skin wound healing.[74,75] In combination with the observation in change of SHIM signal, the decrease in diameter of these constructs has been evaluated. The measured diameters are reported in Figure S5A, Supporting Information. Similarly to reports for fibroblasts,[76] collagen hydrogels containing the lowest collagen concentration contracted the most (diameter decrease by 83% for 0.03 wt%

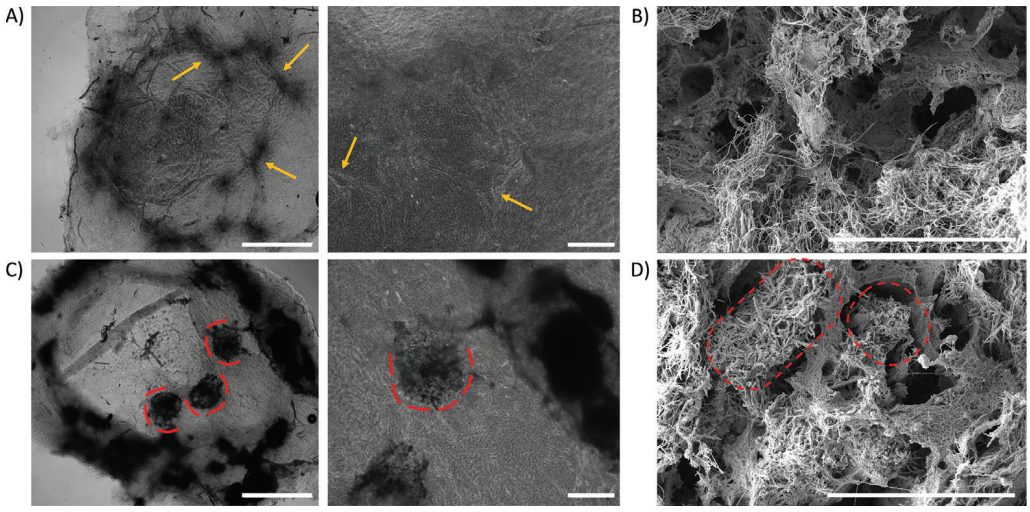

Figure 6. A,C) Phase contrast and B,D) SEM micrographs of constructs after ten days in culture. Phase contrast micrographs of A) Alg and C) AlgCol microspheres show local densification of the collagen matrix in the cell rich areas (visible as dark regions in the image, orange arrows). Red semi-circles highlight the position of former alginate-collagen microspheres. Scale bar left image: 1 mm, Scale bar right image: 250 µm. SEM micrographs of B) Alg and D) AlgCol microspheres. Cells are embedded in collagen fiber hydrogels in (B). For AlgCol microspheres (D), the remaining collagen fibers after alginate dissolution display a significantly different structure (red circles) compared to the collagen fibers in the surrounding hydrogel matrix. Scale bar 30 µm.

collagen compared to 62% for 0.15 wt% collagen with respect to initial size upon preparation). The increase in intensity of the SHIM signals correlates well with the overall shrinkage of the constructs.

Next, the effect of collagen contraction was compared between the samples prepared with temporal alginate microcarriers. In contrast to the sample containing uniformly distributed cells (Figure S5B, Supporting Information, 0.07 wt% collagen), the samples containing cells released from either alginate (**Figure 6**A) or alginate-collagen (Figure 6C) microspheres do only show a local contraction of the collagen matrix. In both cases, the original locations of the microspheres were still visible. For the sample that has been prepared with alginate microspheres, formation of intracellular network between cells from individual voids is observed and cells migrate into and contract the collagen matrix (Figure 6A). For the sample prepared with alginate-collagen microspheres, the spherical voids are still recognizable after ten days in culture (Figure 6C) and less contraction is observed. Upon collagen fiber contraction, the hydrogel does not only shrink but also becomes non-transparent (Figure S5B, Supporting Information). Similarly, the locally cell-enriched regions in Figure 6A,C are significantly opaquer than the cell-free collagen matrix further away.

In addition, Figure 6B,D show scanning electron microscopy (SEM) micrographs of the collagen matrix for cell-containing, alginate (Figure 6B) and alginate-collagen (Figure 6D) microspheres encapsulated in 0.07 wt% collagen after 10 days in culture. Both micrographs depict a collagen hydrogel structure consisting of long, thin fibers, however, Figure 6D also shows the presence of shorter collagen fibers (red circles) that were originally part of the alginate-collagen composite. This in good agreement with the two distinctively different types of collagen fibers highlighted in the confocal analysis of these samples (Figures 3 and 4A,B).

3. Conclusion and Future Directions

In this work, a new method which enables the fabrication of structurally complex hydrogel constructs with spatially defined cell pockets and without the need of advanced techniques and instrumentation is described. The use of soluble alginate and alginate-collagen microcarriers resulted in the distinct formation of a collagen-containing microenvironment within a larger, differently structured macroenvironment.

The fabricated constructs do not shrink with an increased culture period, making it possible to study artificially engineered constructs over a longer period of time. The facile encapsulation of cells in alginate microspheres allows control over the cell number, initial sphere-size, as well as, the design of the microstructure by adding components such as collagen or other ECM-related components. In future studies, it could also be possible to add molecules such as growth factors to create biochemical gradients at the macroscale. The use of the pre-osteoblast cell line MC3T3-E1 showed that it was possible to create a layered construct with distinct cell-containing regions which migrate into the construct and develop cell–cell contact points to neighboring cells in 3D.

Owing to the simplicity of this method, it is possible to fabricate much more advanced constructs in future studies. This could be done by adding more, ECM-related, biopolymers to the surrounding collagen matrix, introducing additional microspheres containing a second cell population or even introducing gradients by applying several, intrinsically different layers on top of each other. Furthermore, the microstructure of the microspheres themselves can be modified, creating cell-specific pockets which could, besides biopolymers such as, collagen, contain biochemical molecules which consequently will also introduce a chemical gradient in the whole system. These are only a handful of possible, future applications than can be done regarding

developing an advanced 3D system which contains cell pockets and could express physical, as well as, biochemical cues to facilitate cell migration and development.

4. Experimental Section

Chemicals: All chemicals were purchased from Sigma-Aldrich unless stated otherwise. De-ionized milli-Q water (MQ-water, 18.2 $M\Omega cm^{-1}$) was used throughout the experiments. Sodium alginate (Protanal LF200S, FMC Biopolymers, $M_W = 2.74 \times 10^5$ g •mol^{-1}, fraction of G-monomers: $F_G = 0.68$) was used for the microsphere preparation. Rat tail collagen type I used in this study was purchased from ThermoFisher Scientific (3 mg mL^{-1}, catalogue number: A1048301). For the preparation of the collagen precursor solution, the manufacturers protocol was followed but PBS was exchanged with 0.1 M MOPS, pH 7.4. Concentrations of alginate and collagen solutions were adjusted using ascorbic acid-free cell media (ThermoFisher Scientific, α-MEM no ascorbic acid, catalogue number: A1049001; supplemented with 10% fetal bovine serum, 0.5% 200 mM L-Glutamate, 1% Gentamicin).

Cell Culture and Preparation of Alginate- and Alginate-Collagen Microspheres: MC3T3-E1 (subclone 4) cells were cultured and expanded in ascorbic acid-free cell media. Prior to the incorporation of cells in alginate and alginate-collagen microspheres, the cells were stained with 35 µM CellTracker Blue (CMF2HC, ThermoFisher Scientific) in suspension for 40 min at 37 °C in serum-free cell media. Cells were centrifuged and resuspended in fresh cell culture media before combining them with 0.6 weight per volume (wt)% alginate or 0.6 wt% alginate—0.07 wt% collagen precursor solution in a syringe. The collagen precursor solution was prepared according to the manufacturers protocol but with exchanging the PBS with 0.1 MOPS, pH 7.4. The syringe was mounted in a microfluidic pump. The microspheres were prepared using an in-house electrostatic droplet generator, with a nozzle size of 0.35 mm, operating at 7 kV, a gelling bath containing 50 mM calcium chloride ($CaCl_2$), 50 mM sodium chloride (NaCl), and 10 mM Tris (hydroxymethyl)-aminomethane (TRIS) at pH 7.3 and a flow of 55 mL h^{-1}. Upon contact of the cell-containing alginate- and alginate-collagen solutions with the gelling bath, the calcium ions crosslinked the alginate and, hence, encapsulating the cells in generated alginate- and alginate-collagen microspheres. Microspheres were collected using a pluriStrainer (pluriSelect Life Science, Germany) with a mesh size of 100 µm and transferred to culture media.

Fabrication of Spatially Confined, Cell-Enriched Regions in Collagen Hydrogels: Silicon isolator sheets (Grace Bio-Labs, catalogue number: GBL665201, Merck) were used as a mold during the preparation of the collagen gels. Each well (8.5 mm diameter, 1.7 mm depth) was separately cut from the template and placed in a glass-bottom 12-wellplate (0.17 mm cover glass thickness, #1.5H, P12-1.5H-N, Cellvis) with the adhesive side facing down. In this mold, a first, thin layer of 0.07 wt% collagen was deposited (50 µL). For the preparation of the collagen precursor solution, the protocol as described in the "Chemicals" sub-section was followed. The collagen fibers assembled for 2 h in a humidified atmosphere at 37 °C. For the second layer, the collagen solution was prepared in a similar manner as the first layer but containing additional cell-alginate or cell-alginate-collagen microspheres. After the deposition of the second layer (120 µL) the whole construct gelled for 3 h in a humidified atmosphere at 37 °C before adding ascorbic acid-free cell media. Each sample contained 5 to 8 microspheres. One day after the preparation of the collagen construct, the alginate hydrogel was dissolved using pre-warmed 50 mM ethylenediaminetetraacetic acid (EDTA, pH 8.0, Invitrogen) in PBS, pH 7.4, for 10 min. The samples were afterward immersed in ascorbic acid-free cell media.

Fabrication of Cell-Containing Collagen Hydrogels: Collagen hydrogels that contained suspended cells were prepared in a similar manner, adding cells at a concentration of 50 000 cells mL^{-1}. The gels were left to solidify for 3 h at 37 °C and 5% CO_2, afterward, ascorbic acid-free cell media was added.

Evaluation of Cell Development and Their Interaction with the Collagen Hydrogel Matrix: The interaction of the cells with the surrounding collagen matrix was studied by SHIM of the assembled collagen fibers and CLSM using a TSC SP8MP microscope (Leica Microsystems). The microscope was equipped with standard photomultiplier tubes (PMT's) and hybrid detectors (HyD's). White light laser (WLL, Leica Microsystems, Imaging Laser WLLPP) and a tunable, near-infrared laser Chameleon Vision-S (Coherent) was used. All samples have been imaged using a 25x water objective, NA = 0.95.

Prior the collagen hydrogel preparation, all cells were incubated with Cell Tracker Blue (CTB), a long-term fluorescent stain that is retained in the cytosol. However, after 72–96 h, the stain started to fade. Hence, the cells were additionally stained with a Deep Red Plasma Membrane stain (DRPM) prior imaging from day 4 onward. Briefly, the CellMask stain (ThermoFisher Scientific, catalog number: C10046) was diluted 1:1000 in pre-warmed PBS, pH 7.4, added to the samples and incubated for 30 min before adding culture media. To simultaneously collect the second harmonic generated SHIM and the 2-photon fluorescent signal from CTB, the wavelength of the multiphoton laser was set to 765 nm. The SHIM signal was detected using an external HyD detector in the range of 370–410 nm. For the CTB signal, the signal was detected with an external HyD detector in the range of 435–455 nm. The laser power was minimized to prevent sample damage. The fluorescent signal of the DRPM stain was excited using a WLL at 649 nm and the emitted signal was collected with an internal PMT. All images were taken with a frame size of 1024 × 1024, an imaging speed of 100 Hz and a line average of 12. For illustration purposes, a MATLAB program was used for image processing, including background removal and brightness/contrast adjustments.

Control samples of undissolved alginate and alginate-collagen microspheres in a collagen hydrogel were stained after 10 days with 2 µM Calcein-AM and 4 µM ethidium homodimer-1 (LIVE/DEAD Viability/Cytotoxicity Kit, Molecular Probes) in pre-warmed PBS, 40 min at 37 °C and 5% CO_2 for their live and dead cell content, respectively.

Characterization of Microspheres Prior Alginate Dissolution: After microsphere preparation, the samples were imaged using an Andor Zyla SCMOS camera attached to a Nikon Eclipse TS100 microscope. Images were taken using a 10x/0.3 Nikon Plan Fluor phase contrast objective. The diameters were measured with the software ImageJ after calibration with a calibration slide. The containing cells were counted manually. Plots were prepared using Origin8 Pro Software.

Time-Series Documentation of Alginate Dissolution: A Nikon Eclipse TS100 microscope with an attached Andor Zyla SCMOS camera was used to record videos from the de-gelling of the alginate component. The samples were brought in focus using a 10x/0.3 Nikon Plan Fluor phase contrast objective. The de-gelling was induced with 100 µL of 50 mM EDTA in PBS, pH 7.4.

Sample Preparation for Scanning Electron Microscopy: After 10 days of culture, the samples were fixated using 4% paraformaldehyde in PBS, pH 7.4 for 6 h. The fixation solution was removed, and the samples were washed once with PBS. A solution containing a total of 2.5 wt% agarose in MQ-water was added and the samples were placed in an oven, set to 80 °C in a humidified environment. After 30 min, the samples were taken out of the oven and the dissolved agarose cooled down to room temperature with constant shaking using a roller mixer SRT6D (20 rpm, stuart BioCote). The embedded samples were then cut into thin, 150 µm slices using a vibratome (Leica VT1000S). The cut samples were dried using a critical point dryer (Quorum K850). Prior imaging with a SEM APREO system (ThermoFisher Scientific), the samples were coated with 12.5 nm of platin/palladium (Pt/Pd, 80/20). The imaging was conducted at 1 kV, 6.3 pA, and an additional bias set to 50 V to prevent surface charging and damaging.

Supporting Information

Supporting Information is available from the Wiley Online Library or from the author.

Acknowledgements

The authors thank the Research Council of Norway, project number 262893, for financial support under the FRINATEK program. Furthermore, the Research Council of Norway is acknowledged for the support to the Norwegian Micro- and Nano- Fabrication Facility, NorFab, project number 295864. The microscopic imaging was performed at the Center for Advanced Microscopy, the Norwegian University of Science and Technology (NTNU) with technical assistance from Astrid Bjørkøy. Additionally, the authors would like to thank Ms. Marieke Olsman for her help and expertise with the MATLAB-based image processing steps. Figure 1A and the ToC figure have been created using Biorender.com.

Conflict of Interest

The authors declare no conflict of interest.

Author Contributions

S.L. and P.S. designed the project, S.L. performed the experiments and processed the data. All authors contributed to the manuscript and have approved to the final version of the manuscript.

Data Availability Statement

The data that supports the findings of this study are available from the corresponding author upon reasonable request.

Keywords

cell migration, collagen hydrogel, in vitro, microcarriers, sacrificial alginate, tissue engineering

Received: August 10, 2021
Revised: September 29, 2021
Published online: October 31, 2021

[1] M. A. Meyers, P.-Y. Chen, A. Y.-M. Lin, Y. Seki, *Prog. Mater. Sci.* **2008**, *53*, 1.
[2] R. Florencio-Silva, G. R. D. S. Sasso, E. Sasso-Cerri, M. J. Simões, P. S. Cerri, *Biomed Res. Int.* **2015**, *2015*, 421746.
[3] A. Di Luca, C. Van Blitterswijk, L. Moroni, *Birth Defects Res., Part C* **2015**, *105*, 34.
[4] J. E. Phillips, K. L. Burns, J. M. Le Doux, R. E. Guldberg, A. J. Garcia, *Proc. Natl. Acad. Sci. U. S. A.* **2008**, *105*, 12170.
[5] D. A. C. Walma, K. M. Yamada, *Development* **2020**, *147*, dev175596.
[6] A. D. Theocharis, S. S. Skandalis, C. Gialeli, N. K. Karamanos, *Adv. Drug Delivery Rev.* **2016**, *97*, 4.
[7] J. Taipale, J. Keski-Oja, *FASEB J.* **1997**, *11*, 51.
[8] T. H. Barker, *Biomaterials* **2011**, *32*, 4211.
[9] S. Ravindran, A. George, *Exp. Cell Res.* **2014**, *325*, 148.
[10] H. Li, J. M. Mattson, Y. Zhang, *J. Mech. Behav. Biomed. Mater.* **2019**, *92*, 1.
[11] R. J. Wade, J. A. Burdick, *Mater. Today* **2012**, *15*, 454.
[12] A. Khademhosseini, R. Langer, *Nat. Protoc.* **2016**, *11*, 1775.
[13] L. G. Griffith, G. Naughton, *Science* **2002**, *295*, 1009.
[14] G. Jensen, C. Morrill, Y. Huang, *Acta Pharm. Sin. B* **2018**, *8*, 756.
[15] O. Jeon, D. S. Alt, S. W. Linderman, E. Alsberg, *Adv. Mater.* **2013**, *25*, 6366.
[16] P. Lu, K. Takai, V. M. Weaver, Z. Werb, *Cold Spring Harbor Perspect. Biol.* **2011**, *3*, a005058.
[17] P. Romani, I. Brian, G. Santinon, A. Pocaterra, M. Audano, S. Pedretti, S. Mathieu, M. Forcato, S. Bicciato, J.-B. Manneville, N. Mitro, S. Dupont, *Nat. Cell Biol.* **2019**, *21*, 338.
[18] H. C. Chen, *Methods Mol. Biol.* **2005**, *294*, 15.
[19] N. S. Brown, R. Bicknell, in *Metastasis Research Protocols* (Eds: S. A. Brooks, U. Schumacher), Humana Press, Totowa, NJ **2003**, pp. 47–54.
[20] R. B. Dickinson, J. B. Mccarthy, R. T. Tranquillo, *Ann. Biomed. Eng.* **1993**, *21*, 679.
[21] S. Yamada, S. Toda, T. Shin, H. Sugihara, *Arch. Otolaryngol., Head Neck Surg.* **1999**, *125*, 424.
[22] A. Autissier, C. L. Visage, C. Pouzet, F. Chaubet, D. Letourneur, *Acta Biomater.* **2010**, *6*, 3640.
[23] B. Leukers, H. Gülkan, S. H. Irsen, S. Milz, C. Tille, M. Schieker, H. Seitz, *J. Mater. Sci.: Mater. Med.* **2005**, *16*, 1121.
[24] R. B. Vernon, E. H. Sage, *Microvasc. Res.* **1999**, *57*, 118.
[25] R. B. Vernon, M. D. Gooden, *Matrix Biol.* **2002**, *21*, 661.
[26] D. W. Levine, J. S. Wong, D. I. C. Wang, W. G. Thilly, *Somatic Cell Genet.* **1977**, *3*, 149.
[27] S. Tielens, H. Declercq, T. Gorski, E. Lippens, E. Schacht, M. Cornelissen, *Biomacromolecules* **2007**, *8*, 825.
[28] V. Nehls, D. Drenckhahn, *Microvasc. Res.* **1995**, *50*, 311.
[29] J. L. Drury, D. J. Mooney, *Biomaterials* **2003**, *24*, 4337.
[30] M. W. Tibbitt, K. S. Anseth, *Biotechnol. Bioeng.* **2009**, *103*, 655.
[31] S. R. Peyton, C. B. Raub, V. P. Keschrumrus, A. J. Putnam, *Biomaterials* **2006**, *27*, 4881.
[32] A. Skardal, L. Smith, S. Bharadwaj, A. Atala, S. Soker, Y. Zhang, *Biomaterials* **2012**, *33*, 4565.
[33] K. Y. Lee, D. J. Mooney, *Chem. Rev.* **2001**, *101*, 1869.
[34] M. R. Singh, S. Patel, D. Singh, in *Nanobiomaterials in Soft Tissue Engineering: Applications of Nanobiomaterials* (Ed: A. M. Grumezescu), Elsevier Inc., Amsterdam **2016**, pp. 231–260.
[35] H. Tan, K. G. Marra, *Materials* **2010**, *3*, 1746.
[36] G. D. Nicodemus, S. J. Bryant, *Tissue Engineering Part B: Reviews* **2008**, *14*, 149.
[37] W.-H. Tan, S. Takeuchi, *Adv. Mater.* **2007**, *19*, 2696.
[38] I. Ghidoni, T. Chlapanidas, M. Bucco, F. Crovato, M. Marazzi, D. Vigo, M. L. Torre, M. Faustini, *Cytotechnology* **2008**, *58*, 49.
[39] B. Sarker, J. Rompf, R. Silva, N. Lang, R. Detsch, J. Kaschta, B. Fabry, A. R. Boccaccini, *Int. J. Biol. Macromol.* **2015**, *78*, 72.
[40] L. Cao, W. Lu, A. Mata, K. Nishinari, Y. Fang, *Carbohydr. Polym.* **2020**, *242*, 116389.
[41] Y. Fang, S. Al-Assaf, G. O. Phillips, K. Nishinari, T. Funami, P. A. Williams, L. Li, *J. Phys. Chem. B* **2007**, *111*, 2456.
[42] K. E. Kadler, C. Baldock, J. Bella, R. P. Boot-Handford, *J. Cell Sci.* **2007**, *120*, 1955.
[43] K. Gelse, E. Pöschl, T. Aigner, *Adv. Drug Delivery Rev.* **2003**, *55*, 1531.
[44] A. Sorushanova, L. M. Delgado, Z. Wu, N. Shologu, A. Kshirsagar, R. Raghunath, A. M. Mullen, Y. Bayon, A. Pandit, M. Raghunath, D. I. Zeugolis, *Adv. Mater.* **2019**, *31*, 1801651.
[45] A. M. Ferreira, P. Gentile, V. Chiono, G. Ciardelli, *Acta Biomater.* **2012**, *8*, 3191.
[46] F. H. Silver, D. E. Birk, *Top. Catal.* **1983**, *3*, 393.
[47] M. Achilli, D. Mantovani, *Polymers* **2010**, *2*, 664.
[48] J. R. Harris, A. Soliakov, R. J. Lewis, *Micron* **2013**, *49*, 60.
[49] Y. Li, A. Asadi, M. R. Monroe, E. P. Douglas, *Mater. Sci. Eng., C* **2009**, *29*, 1643.
[50] A. Arslan-Yildiz, R. E. Assal, P. Chen, S. Guven, F. Inci, U. Demirci, *Biofabrication* **2016**, *8*, 014103.
[51] S. Zhang, H. Wang, *SLAS Technol.* **2019**, *24*, 70.
[52] F. Pati, J. Gantelius, H. A. Svahn, *Angew. Chem., Int. Ed.* **2016**, *55*, 4650.

[53] Z. Zhang, Y. Jin, J. Yin, C. Xu, R. Xiong, K. Christensen, B. R. Ringeisen, D. B. Chrisey, Y. Huang, *Appl. Phys. Rev.* **2018**, *5*, 041304.
[54] B. Guillotin, A. Souquet, S. Catros, M. Duocastella, B. Pippenger, S. Bellance, R. Bareille, M. Rémy, L. Bordenave, J. Amédée, F. Guillemot, *Biomaterials* **2010**, *31*, 7250.
[55] Z. Fu, S. Naghieh, C. Xu, C. Wang, W. Sun, X. Chen, *Biofabrication* **2021**, *13*, 033001.
[56] K. Dubbin, A. Tabet, S. C. Heilshorn, *Biofabrication* **2017**, *9*, 044102.
[57] D. Chimene, K. K. Lennox, R. R. Kaunas, A. K. Gaharwar, *Ann. Biomed. Eng.* **2016**, *44*, 2090.
[58] N. Ashammakhi, S. Ahadian, C. Xu, H. Montazerian, H. Ko, R. Nasiri, N. Barros, A. Khademhosseini, *Mater. Today Bio* **2019**, *1*, 100008.
[59] M. De Groot, H. G. D. Leuvenink, P. P. M. Keizer, S. Fekken, T. A. Schuurs, R. Van Schilfgaarde, *J. Biomed. Mater. Res., Part A* **2003**, *67A*, 679.
[60] J. Cohen, K. L. Zaleski, G. Nourissat, T. P. Julien, M. A. Randolph, M. J. Yaremchuk, *J. Biomed. Mater. Res., Part A* **2011**, *96A*, 93.
[61] N. V. Ballal, M. Kundabala, S. Bhat, N. Rao, B. S. S. Rao, *Oral Surg., Oral Med., Oral Pathol., Oral Radiol., Endodontol.* **2009**, *108*, 633.
[62] J. S. R. Marins, L. M. Sassone, S. R. Fidel, D. A. Ribeiro, *Braz. Dent. J.* **2012**, *23*, 527.
[63] C.-Y. Chen, C.-J. Ke, K.-C. Yen, H.-C. Hsieh, J.-S. Sun, F.-H. Lin, *Theranostics* **2015**, *5*, 643.
[64] Y.-J. Lin, C.-N. Yen, Y.-C. Hu, Y.-C. Wu, C.-J. Liao, I.-M. Chu, *J. Biomed. Mater. Res., Part A* **2009**, *88A*, 23.
[65] F. D. Ceuninck, C. Lesur, P. Pastoureau, A. Caliez, M. Sabatini, *Methods Mol. Med.* **2004**, *100*, 15.
[66] B. D. Plouffe, M. A. Brown, R. K. Iyer, M. Radisic, S. K. Murthy, *Lab Chip* **2009**, *9*, 1507.
[67] C. Aimé, M.-C. Schanne-Klein, S. Bancelin, T. Coradin, *Biomed. Opt. Express* **2012**, *3*, 1446.
[68] V. Lutz, M. Sattler, S. Gallinat, H. Wenck, R. Poertner, F. Fischer, *Int. J. Cosmet. Sci.* **2012**, *34*, 209.
[69] G. Cox, E. Kable, A. Jones, I. Fraser, F. Manconi, M. D. Gorrell, *J. Struct. Biol.* **2003**, *141*, 53.
[70] C. G. Fuentes-Corona, J. Licea-Rodriguez, R. Younger, R. Rangel-Rojo, E. O. Potma, I. Rocha-Mendoza, *Biomed. Opt. Express* **2019**, *10*, 6449.
[71] S. Lehnert, P. Sikorski, *Mater. Sci. Eng., C* **2021**, *121*, 111840.
[72] V. Lutz, M. Sattler, S. Gallinat, H. Wenck, R. Poertner, F. Fischer, *Skin Res. Technol.* **2012**, *18*, 168.
[73] M. Eastwood, R. Porter, U. Khan, G. Mcgrouther, R. Brown, *J. Cell. Physiol.* **1996**, *166*, 33.
[74] R. Montesano, L. Orci, *Proc. Natl. Acad. Sci. U. S. A.* **1988**, *85*, 4894.
[75] H. P. Ehrlich, J. B. M. Rajaratnam, *Tissue Cell* **1990**, *22*, 407.
[76] Y. K. Zhu, T. Umino, X. D. Liu, H. J. Wang, D. J. Romberger, J. R. Spurzem, S. I. Rennard, *In Vitro Cell. Dev. Biol.: Anim.* **2001**, *37*, 10.